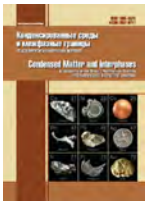

ISSN 1606-867X (Print)
ISSN 2687-0711 (Onine)
Condensed Matter and Interphases
Kondensirovannye Sredy i Mezhfaznye Granitsy
https://journals.vsu.ru/kcmf/

Original articles

Original article
https://doi.org/10.17308/kcmf.2021.23/3305

Calculation of the nonstoichiometry area of nanocrystalline palladium (II) oxide films

A. M. Samoylov✉, D. I. Pelipenko, N. S. Kuralenko

[2]Voronezh State University,
1 Universitetskaya pl., Voronezh 394018, Russian Federation

Abstract

Nanocrystalline palladium (II) oxide films were synthesised using thermal oxidation in the oxygen atmosphere of the initial ultradispersed metal palladium layers with a thickness of ~ 35 nanometres that were obtained on SiO_2/Si (100) substrates using the method of thermal sublimation in high vacuum. Using X-ray analysis, it was established that during thermal oxidation in the oxygen atmosphere within the temperature range T = 670–970 K the values of the a and c parameters of the tetragonal lattice as well as the unit cell volume of nanocrystalline PdO films increased monotonously with the rise of the temperature reaching the maximum values at T = 950–970 K. It was found that the parameters of the tetragonal lattice and the unit cell volume of nanocrystalline PdO films decreased as the oxidation temperature increased up to T > 970 K Based on the ratio of the c/a parameters, it was shown that the main contribution to the deformation phenomena of the tetragonal lattice were mostly due to the increase in the elementary translations along the coordination axes OX and OY. Based on an assumption that the ionic component of the chemical bond is essential to the palladium (II) oxide structure, we suggested a method for the calculation of the range of the nonstoichiometry area for nanocrystalline PdO films, using the reported data on the radii of cation Pd^{2+} and anion O^{2-} taking into account their coordination environment. The results of the calculations showed that nanocrystalline PdO films synthesised with an oxygen pressure of ~ 105 kPa are characterised by the two-sided homogeneity region in relation to the stoichiometric ratio of the components. The homogeneity region of nanocrystalline PdO films is characterised by the retrograde solidus line in the range of the temperatures T = 770–1070 K.

Keywords: Palladium (II) oxide, Nanostructures, Thermal oxidation, Crystal structure, Nonstoichiometry, Point defects, Gas sensors

Acknowledgements: the work was supported by the Ministry of Science and Higher Education of the Russian Federation in the framework of the government order to higher education institutions in the sphere of scientific research for years 2020-2022, project No. FZGU-2020-0036.

For citation: Samoylov A. M., Pelipenko D. I., Kuralenko N. S. Calculation of the nonstoichiometry area of nanocrystalline palladium (II) oxide films *Kondensirovannye sredy i mezhfaznye granitsy = Condensed Matter and Interphases*. 2021;23(1): 62–72. https://doi.org/10.17308/kcmf.2021.23/3305

Для цитирования: Самойлов А. М., Пелипенко Д. И, Кураленко Н. С. Расчет области нестехиометрии нанокристаллических пленок оксида палладия (II). *Конденсированные среды и межфазные границы*. 2021;23(1): 62–72. https://doi.org/10.17308/kcmf.2021.23/3305

✉ Alexander M. Samoylov, e-mail: samoylov@chem.vsu.ru.

1. Introduction

Gas sensors of various types are designed for the accurate, fast, and reliable determination of concentrations of toxic and explosive gases in the atmospheric air [1–3]. Such devices are necessary for the prevention of technological and household incidents with explosive gases, as well as for security systems in different industrial processes that use poisonous or flammable volatile substances [1–4]. The creation of effective resistive gas sensors based on wide-band metal oxide semiconductors is a relevant scientific and technical task as it will allow producing portable individual devices [5–7]. Over the past fifty years, metal oxide semiconductors with *n*-type conductivity have been the main objects of research and development, and tin dioxide SnO_2 has undoubtedly been the leader among them [1–3, 5, 6].

Impressive success in the development of sensors based on *n*-type semiconductors can be explained by the results of studying the physicochemical patterns that describe and predict the nature of the interaction of the active layer surface with the molecules of detected gases [3–4, 8]. It was established that *n*-type wide-band semiconductors, particularly SnO_2, are characterised by a rather narrow homogeneity region [1, 5–6, 8]. As we know [1–2, 3, 9], point defects are highly significant in the interaction of the surface of *n*-type semiconductors with the molecules of the analysed gases. Various authors have proved the nature of point defects, mainly oxygen vacancies, which are responsible for nonstoichiometry and electronic type of conductivity of these compounds [1, 5–6, 8, 9].

Over the past decade, there has been a considerable increase in the interest in the study of sensory properties of wide-band metal oxide semiconductors with the *p*-type surface and the composites based on them [10]. So far, the functional properties of metal oxide semiconductors with *p*-type conductivity, such as Cr_2O_3, Cu_2O, PdO, etc., have been studied only partially despite the fact that these materials possess great potential when being used in gas sensors [10]. In a number of publications, it was suggested that metal oxide semiconductors with the *p*-type conductivity would be highly effective for the detection of such toxic gases as ozone, chlorine, nitrogen oxide, and sulphur dioxide [10].

The gas-sensitive properties of nanostructures based on palladium (II) oxide, which is characterised by *p*-type conductivity [11, 12], have only recently become the object of studies. Over the past five years, it has been experimentally proved that nanostructures with different morphological organisation based on palladium (II) oxide possess high sensitivity, sensory response stability, short recovery period, as well as good reproducibility of the sensor signal when detecting hydrogen, carbon monoxide, vapours of organic compounds, nitrogen (IV) oxide, and ozone in the atmospheric air [12 –18].

However, as the analysis of the literature shows, unlike wide-band metal oxide materials with *n*-type conductivity, the phase diagram of palladium – oxide system has not been thoroughly studied, and the homogeneity region of palladium (II) oxide has not been experimentally determined so far [18, 19]. In addition, authors express different opinions on the nature of point defects in this compound [12, 18, 20]. The lack of this information makes it impossible to establish the mechanisms of interaction of the detected gases with the surface of nanostructures of palladium (II) oxide and largely hinders the practical application of gas sensors based on them.

Therefore, the aim of this work was to calculate the range of the nonstoichiometry area of nanocrystalline palladium (II) oxide films based on experimental X-ray diffraction data on the change in the parameters of the tetragonal crystal lattice depending on the conditions of their synthesis.

2. Experimental

A two-stage process was used to synthesise nanocrystalline films of palladium (II) oxide in the present work. During the first stage, using thermal sublimation of palladium foil with a purity of 99.98% in high vacuum (residual pressure in the reaction chamber ~ 10^{-5} Pa), initial microdispersed Pd films were obtained on Si (100) substrates with a buffer layer of the SiO_2 oxide with a thickness of d ~ 300 nm without heating. The method of formation of thin and ultrathin layers of metallic Pd was described in detail in previous works [11, 13–16].

As was established in [20], thermal oxidation of initial ultradispersed layers of metallic Pd in

dry oxygen in the temperature range of T_{ox} = 670–1070 K leads to the formation of single-phase PdO nanocrystalline films. Taking into account the experimental data [20], in the present work the initial heterostructures Pd/SiO_2/Si (100) were thermally oxidised in a dry oxygen atmosphere at a pressure of $p(O_2) \sim 1.1 \cdot 10^5$ Pa in the continuous flow mode with the oxygen consumption of 5 dm^3 per hour. The Pd/SiO_2/Si (100) heterostructures were kept at temperatures T_{ox} = 570, 670, 770, 870, 1070, and 1120 K for 2 hours and then cooled to room temperature in a dry oxygen stream.

The change in the phase composition and crystal lattice parameters of palladium (II) oxide synthesised using thermal oxidation of Pd/SiO_2/Si (100) heterostructures was characterized using X-ray diffractometry on DRON-4-07 and Philips PANanalitical X'Pert devices with CuK_α and CoK_α–radiation. Diffraction patterns of the samples were registered with rotation of the samples, while the profiles of X-ray reflections were constructed pointwise with the step of the counter being 0.01°. The clearly recorded reflection (400) of the Si (100) substrate served as an internal standard to prevent accidental errors.

Precise determination of the tetragonal crystal lattice period of palladium (II) oxide films was conducted by extrapolating the diffraction angle to θ = 90 degrees. For this, an extrapolation function $f(\theta)$ was chosen so that the dependence of parameters a and c on the value of $f(\theta)$ was closest to linear. The best results were obtained using the Nelson-Riley extrapolation function [21]. The lattice constants a and c of the tetragonal structure of nanocrystalline PdO films were calculated using the MATHCAD 10 software based on an algorithm for solving a system of quadratic equations with two non-obvious parameters. The desired value of the lattice parameters a_0 and c_0 were obtained using linear function approximation:

$$a = k \times f(\sin\theta) + a_0 \quad (1\,a)$$

$$c = k \times f(\sin\theta) + c_0 \quad (1\,b)$$

using the least-squares method.

The values of the parameters a and c of the tetragonal crystal lattice of nanocrystalline PdO films calculated on the basis of the obtained experimental X-ray diffraction data, depending on the oxidation temperature T_{ox}, are shown in figs. 1a and 1b as compared to the values of the lattice parameters of the ASTM standard [22, 23]. It must be emphasised that heterophase PdO + Pd films were synthesised as a result of oxidation of the initial ultradispersed films of metal Pd at T_{ox} = 570 K and T_{ox} = 1120 K. The samples synthesised at T_{ox} = 570 K should be considered as products of incomplete transformation of the initial Pd layers into PdO oxide, while the samples obtained at T_{ox} = 1120 K are products of the partial thermal decomposition of nanocrystalline PdO films. The authors [20] indicated that there were reflections on the diffraction patterns of the films synthesised at T_{ox} = 1120 K which could

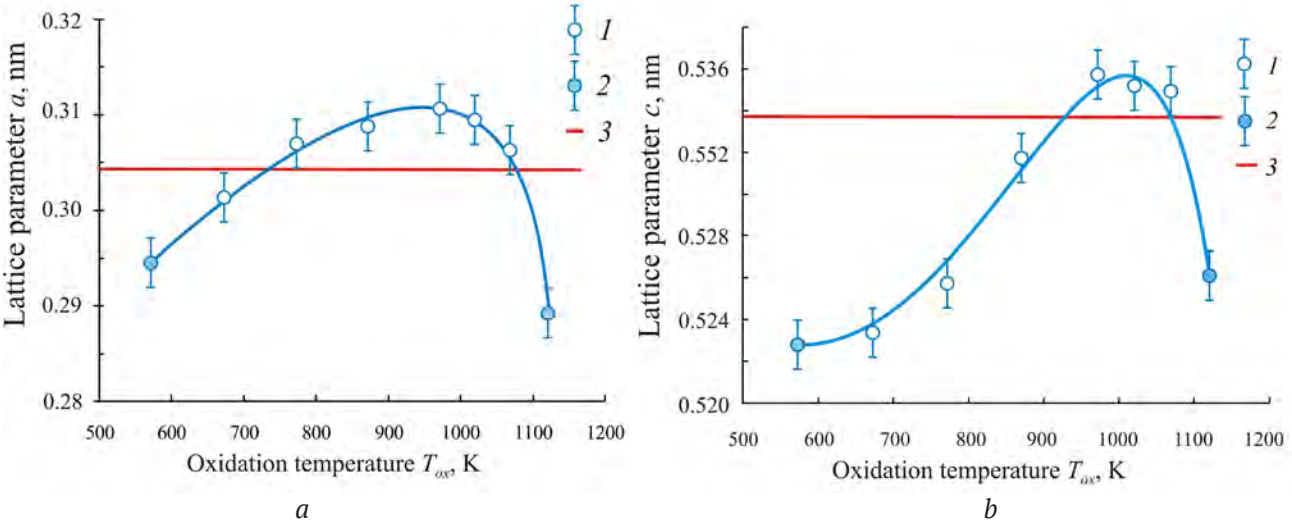

a *b*

Fig. 1. Dependences of the parameters a and c of the tetragonal lattice of nanocrystalline PdO films on the oxidation temperature T_{ox}: *1* – homogeneous PdO films, *2* – heterogeneous PdO + Pd films; *3* – data of the ASTM standard [22, 23]

correspond to the structure of palladium (I) oxide Pd_2O [24]. Nevertheless, the formation of Pd_2O cannot be considered fully proved. The number of low-intensity reflections established in this work is insufficient for the accurate identification of the phase.

As Fig. 1a and Fig. 1b show, the dependencies $a = f(T_{ox})$ and $c = f(T_{ox})$ for nanocrystalline PdO films are characterised by similar behaviour: the values of both parameters monotonously increase with an increase in the oxidation temperature up to T_{ox} = 970 K, and with a further increase in T_{ox} > 970 K their sharp decrease is observed. In this case, the values of the lattice constant a of nanocrystalline PdO films for the temperature range T_{ox} = 770–1070 K, is higher than the value of the similar parameter of the ASTM standard [23] (Fig. 1a). The range of oxidation temperatures where the values of parameter c is higher than the values of the ASTM standard is more specific: from T_{ox} = 870 K to T_{ox} = 1070 K (Fig. 1b). It should be noted that heterogeneous nanocrystalline PdO films obtained at T_{ox} = 570 K and T_{ox} = 1120 K are characterised by the minimal values of the parameters of the tetragonal lattice (Fig. 1a and Fig. 1b).

The results of the calculations of the values of the tetragonal lattice parameters (Fig. 1a and Fig. 1b) indicate that the structure of nanocrystalline PdO is considerably transformed when the space group remains unchanged during thermal oxidation.

In this work, the values of the ratio of the c/a parameters were calculated for a more accurate estimate of the contribution of changes in the a and c parameters to the overall picture of deformation phenomena in the tetragonal lattice of nanocrystalline PdO films. It is known that the c/a ratio is a parametric feature of crystals of the middle category and it reflects the degree of anisotropy of the crystal structure and a number of physical properties [25].

The change in the c/a values for nanocrystalline PdO films depending on the oxidation temperature T_{ox} is presented in Fig. 2. As the figure shows, the c/a values for all single-phase nanocrystalline PdO films obtained by oxidation in oxygen in the temperature range 600 < T_{ox} <1050 K are significantly lower than the value calculated for the reference sample from the ASTM database [23]. On the contrary, the c/a values are higher than the similar value of the reference sample for heterogeneous samples (PdO + Pd) and (PdO + Pd + Pd_2O).

There is a flat minimum in the temperature range 800 < T_{ox} <850 K on the $c/a = f(T_{ox})$ curve presented in Fig. 2. The established nature of the behaviour of the $c/a = f(T_{ox})$ curve indicates that the increase in the tetragonal lattice parameters of nanocrystalline PdO films is uneven. The main contribution to the distortions of the tetragonal crystal structure of palladium (II) oxide occurs mainly due to an increase in the values of

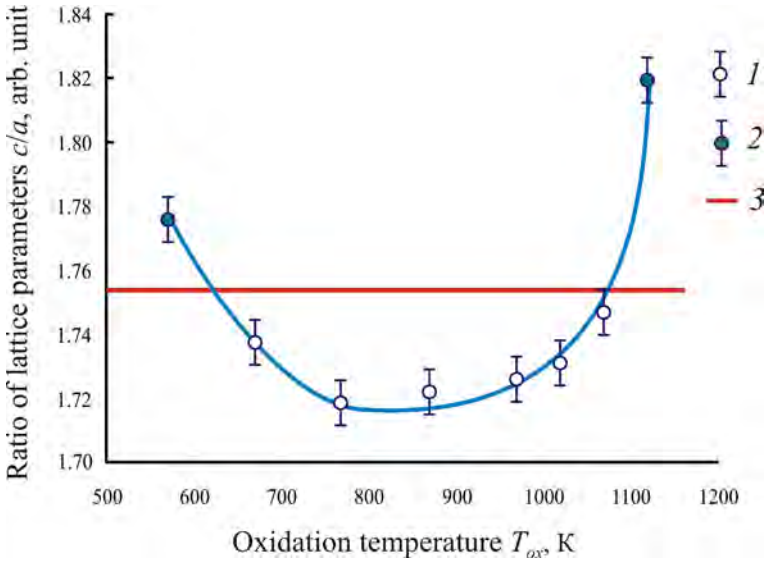

Fig. 2. Dependence of the c/a ratio of the parameters of the tetragonal lattice of nanocrystalline PdO films on the oxidation temperature T_{ox}: *1* – homogeneous polycrystalline PdO samples; *2* – heterogeneous polycrystalline (PdO + Pd) samples; *3* – data of the ASTM standard [23]

the *a* parameter, that is due to an increase in elementary translations along the *OX* and *OY* coordinate axes. Thus, the deformation of the tetragonal crystal structure of nanocrystalline PdO films observed in the oxidation temperature range 670 < T_{ox} < 1070 K is accompanied by a decrease in the values of the parametric ratio *c*/*a*, which leads to a reduction in the degree of anisotropy of the crystal structure.

An analysis of the nature of the transformation of the tetragonal structure of nanocrystalline PdO films during their synthesis needs to be complemented with the calculations of the unit cell volume of the crystal structure using the formula:

$$V_{uc} = a^2 c\,, \qquad (2)$$

where V_{uc} – is the unit cell volume; *a* and *c* – are parameters of the tetragonal crystal structure of palladium (II) oxide. Such calculations allow assessing the average degree of distortion of the tetragonal structure of nanocrystalline PdO films depending on the oxidation temperature due to changes in the values of both parameters *a* and *c*.

The results of the calculations are presented in Fig. 3 as a dependence $V_{uc} = f(T_{ox})$. As the figure shows, the unit cell volume V_{uc} of the crystal structure of single-phase nanocrystalline films of palladium (II) oxide monotonously grow with an increase in the oxidation temperature from

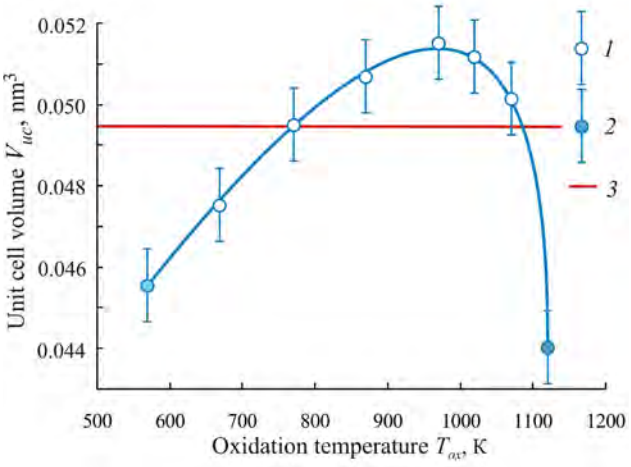

Fig. 3. Dependence of the unit cell volume V_{uc} of the tetragonal lattice of nanocrystalline PdO films on the oxidation temperature T_{ox}: *1* – homogeneous polycrystalline PdO samples; *2* – heterogeneous polycrystalline (PdO + Pd) samples; *3* – data of the ASTM standard [23]

T_{ox} = 670 K to T_{ox} = 970 K. The maximum values of V_{uc} are found in the temperature range 950 < T_{ox} < 970 K. At the same time, in the temperature range T_{ox} = 770 – 1070 K the values of the unit cell volume V_{uc} for homogeneous PdO films exceed the volume of the reference unit cell ASTM [23].

In the present work, the values of the X-ray density were calculated for a fuller picture of the analysis of the deformations in the structure of nanocrystalline PdO films depending on the oxidation temperature. As there are two formula units of palladium (II) oxide in a unit cell [20, 23], the X-ray density ρ_{Xray}(PdO) was calculated using the formula:

$$\rho_{Xray}(\mathrm{PdO}) = \frac{2M(\mathrm{PdO})}{V_{uc} \cdot N_A}, \qquad (3)$$

where *M*(PdO) is the molar mass of palladium (II) oxide; V_{uc} is the unit cell volume; N_A is Avogadro number.

The results of the calculation using formula (3) for palladium (II) oxide of stoichiometric composition in the form of a dependence $\rho_{Xray}(\mathrm{PdO}) = f(T_{ox})$ are presented in Fig. 4. As the figure shows, the values ρ_{Xray}(PdO) monotonously decrease with an increase in the oxidation temperature in the range of 570 < T_{ox} < 970 K. Minimal values of ρ_{Xray}(PdO) were established for the oxidation temperature T_{ox} ~ 970 K Further increase in the oxidation temperature T_{ox} > 970 K is accompanied by a sharp increase in the X-ray density. It should be noted that maximum values of density were obtained for heterogeneous samples (PdO + Pd) and (PdO + Pd + Pd_2O) synthesised at T_{ox} = 570 K and T_{ox} = 1120 K respectively.

The comparison of the obtained experimental data on the change in the tetragonal lattice parameters of nanocrystalline PdO films synthesised at different temperatures (Fig. 1), as well as the calculated dependences of the change in the unit cell volume $V_{uc} = f(T_{ox})$ and X-ray density $\rho_{Xray}(\mathrm{PdO}) = f(T_{ox})$, presented in Fig. 3 and Fig. 4 respectively, indicate that the authors' suggestions [20] about the causes of the distortion of the tetragonal of palladium (II) oxide were appropriate. The increase in the unit cell volume of the PdO tetragonal lattice with an increase in the oxidation temperature at the constant value of oxygen pressure is most likely

due to the incorporation of oxygen atoms into the crystal structure of PdO [20]. It is known [26] that the surface of nanostructures of wide-band metal oxide semiconductors adsorbs oxygen molecules. Moreover, depending on the temperature, the ionisation of the adsorbed molecules of O_2 are observed with the formation of oxygen diatomic and monoatomic anions: O_2^-, O^-, and O^{2-} [26]. The nature of the ionised oxygen particles depends on the temperature [26]. It was shown that double-charged monoatomic anions of oxygen O^{2-} are formed at the temperature of $T_{ox} > 570$ K [26].

The obtained calculation data on the change in the X-ray density ρ_{Xray}(PdO) of nanocrystalline PdO films with an increase in the temperature also support this hypothesis (Fig. 4). A decrease in the values of density ρ_{Xray}(PdO) can be explained by the incorporation of oxygen atoms into the lattice whose atomic mass is 6.6515 times smaller than the mass of palladium atoms:

$$\frac{A_r(\mathrm{O})}{A_r(\mathrm{Pd})} = \frac{15.9994}{106.42} = 0.150342. \quad (4)$$

3. Methodology for the calculation of nonstoichiometry areas

In the present work, based on the obtained experimental and calculation data, we propose a method for the calculation of the range of the nonstoichiometric areas of nanocrystalline PdO films within the above-mentioned hypothesis, which explains the deformation of the crystal lattice depending on the oxidation temperature.

During the calculation of the nonstoichiometric areas of nanocrystalline PdO films, boundary conditions were established and three main assumptions were specified.

1. High proportion of the ionic component of the chemical bond in palladium (II) oxide.

The review of the literature data shows that, as for its chemical properties, palladium (II) oxide is a sparingly soluble basic oxide, similar to MnO, NiO, FeO, etc. [25. 27, 28]. This fact indicates that despite the low values of the coordination numbers in the tetragonal structure: $CN(Pd_O) = CN(O_{Pd}) = 4$, the proportion of the ionic component of the chemical bond in palladium (II) oxide is rather high.

The proportion of the ionic bond in palladium (II) oxide can be assessed using the method

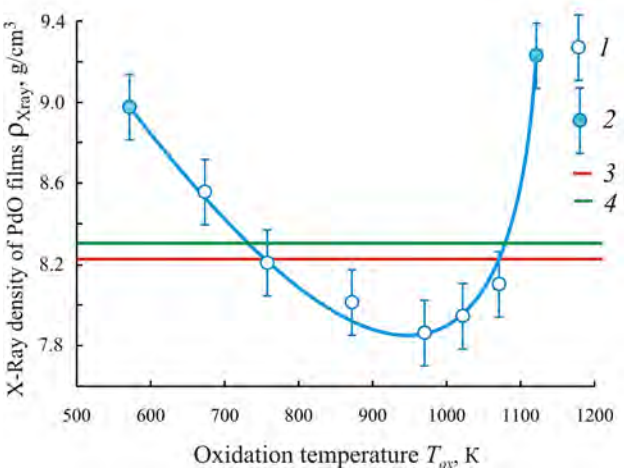

Fig. 4. Dependence of the X-ray density ρ_{Xray} nanocrystalline PdO films on the oxidation temperature T_{ox}: *1* – homogeneous polycrystalline PdO samples; *2* – heterogeneous polycrystalline PdO + Pd samples; *3* – data of the ASTM standard [23]; *4* – density values of polycrystalline PdO samples obtained using the hydrostatic method [26]

proposed by the authors of [29] based on the comparison of the relative electronegativity (ENE) of the elements that form the binary compound of the AB composition. Within this method, an elementary substance with semiconducting properties, for example, single-crystal Si, has a proportion of ionicity equal to zero, while caesium fluoride CsF is characterised by a proportion of ionicity equal to 1 (Fig. 5). The values of relative electronegativity (ENE) of chemical elements that form some binary compounds of the AB composition are presented in Table 1.

A comparison of the values of the relative electronegativity (ENE) of the elements by the Pauling scale [30] is shown (Table 1):

$$\Delta\chi(\mathrm{CsF}) = \chi(\mathrm{F}) - \chi(\mathrm{Cs}) = 3.98 - 0.79 = 3.19 \quad (5\ a)$$

$$\Delta\chi(\mathrm{NaCl}) = \chi(\mathrm{Cl}) - \chi(\mathrm{Na}) = 3.16 - 0.93 = 2.27 \quad (5\ b)$$

$$\Delta\chi(\mathrm{PdO}) = \chi(\mathrm{O}) - \chi(\mathrm{Pd}) = 3.44 - 2.20 = 1.24 \quad (5\ c)$$

Using this method [29] and its graphic interpretation (Fig. 5), it is possible to determine the proportion of the ionic component of the chemical bond in palladium (II) oxide. As Fig. 5 shows, based on the value of the difference between ENE of oxygen and palladium $\Delta\chi$(PdO) = 1.24 calculated using formula (5 c), the proportion of the ionic component of the chemical bond in palladium (II) oxide is approximately 39%.

Table 1. The values of relative electronegativity (ENE) of some chemical elements [30] and the proportion of the ionic component of the chemical bond in binary compounds of the AB composition formed by these elements

Compound	Relative electronegativity of the elements (ENE) χ, r.u.		Difference between ENE elements Δχ, r.u.	Degree of ionicity, r.u.
CsF	χ(Cs) = 0.79	χ(F) = 3.98	Δχ = 3.19	1.0
CsCl	χ(Cs) = 0.79	χ(Cl) = 3.16	Δχ = 2.37	0.76
NaF	χ(Na) = 0.93	χ(F) = 3.98	Δχ = 3.05	0.92
NaCl	χ(Na) = 0.93	χ(Cl) = 3.16	Δχ = 2.23	0.68
MnO	χ(Mn) = 1.55	χ(O) = 3.44	Δχ = 1.89	0.59
PdO	χ(Pd) = 2.20	χ(O) = 3.44	Δχ = 1.24	0.39
ZnO	χ(Zn) = 1.65	χ(O) = 3.44	Δχ = 1.79	0.5
ZnS	χ(Zn) = 1.65	χ(S) = 2.58	Δχ = 0.93	0.28

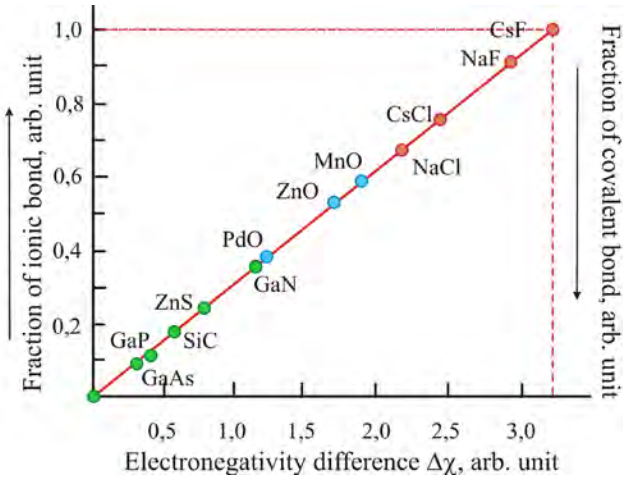

Fig. 5. Dependence of the proportion of the ionic component of the chemical bond in AB binary compounds on the value of the difference between the relative electronegativity of the elements calculated using the method [29]

The obtained values of Δχ(PdO) elements and the value of the proportion of ionicity allow concluding that the chemical bond in palladium (II) oxide is covalent with a significant proportion of the ionic component. Therefore, it is quite reasonable to assume that it is possible to consider palladium and oxygen particles in the crystal structure of palladium (II) oxide as ions with spherical symmetry. For this reason, to conduct the calculations it is reasonable to use the data on the ionic radii of elements $R(Pd^{2+})$ and $R(O^{2-})$ presented in Table 2 [30–32].

2. As a sample of palladium (II) oxide, the composition of which corresponds to the stoichiometric ratio of the components, we used a standard from the ASTM database [23] with the following parameters of the tetragonal lattice: $a = 0.30434$ nm, $c = 0.5337$ nm. Thus, the unit cell volume V_{uc}^0 of the standard sample of PdO can be expressed by the following equation:

$$V_{uc}^0 = 2V(Pd^{2+}) + 2V(O^{2-}) + V_{void}, \quad (6)$$

where $V(Pd^{2+})$ and $V(O^{2-})$ are the volumes of palladium and oxygen anion respectively; V_{viod} is the total volume of the tetrahedral and octahedral voids.

3. To calculate the range of the homogeneity (nonstoichiometry) area of nanocrystalline PdO films, in the present work we used the variant of the unit cell of the crystal structure of palladium (II) oxide suggested in [20]. This variant of the representation of the PdO unit cell (Fig. 6) completely corresponds to the latest experimental data [23], in particular, to a set of elements of the space group symmetry (SGS) $P4_2/mmc$, Pearson symbol $tP4$, Wyckoff position of the atoms of Pd and O, as well as their multiplicity [20, 23].

When calculating the values of deviation from stoichiometry ô of nanocrystalline films of palladium (II) oxide, we used the concept of the "effective volume" of the particles of palladium $V_{eff}(Pd^{2+})$ and oxygen $V_{eff}(O^{2-})$ in a unit cell. The "effective volume" of the particles of palladium and oxygen were determined using the ratio:

$$2V_{eff}(Pd^{2+}) + 2V_{eff}(O^{2-}) = V_{uc}^0, \quad (7)$$

where V_{uc}^0 is the unit cell volume of the standard of the ASTM data [23].

The values of δ were determined when solving the equation system:

Table 2. Values of palladium Pd^{2+} and oxygen O^{2-} ionic radii [30 – 32]

Ion	Coordination number CN	Coordination polyhedron	Values of ionic radii R_{ion}, nm
Pd^{2+}	4	Square (rectangular)	0.078 [30]; 0.086 [31]; 0.078 [32]
O^{2-}	4	Tetragonal tetrahedron	0.132 [30]; 0.140 [31]; 0.124* [31]; 0.132 [32]

*The values of ionic radius were obtained on the basis of quantum mechanical calculations.

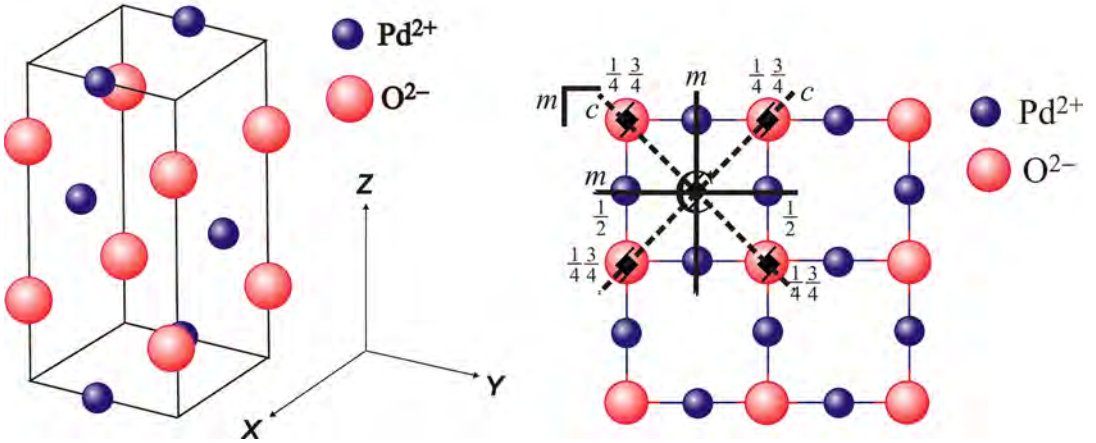

a *b*

Fig. 6. Unit cell of palladium (II) oxide tetragonal crystal structure (a) and projection of four unit cells on *XOY* plane (b) with the indication of the elements of symmetry typical for SG $P4_2/mmc$ [20]

$$\left\{\begin{array}{l} V_{uc}^{0}(T_{ox}) = 2V_{eff}(Pd^{2+}) + 2V_{eff}(O^{2-}) + 2\delta \times V_{eff}(O^{2-}) \\ \dfrac{V_{eff}(Pd^{2+})}{V_{eff}(O^{2-})} = \dfrac{R^3(Pd^{2+})}{R^3(O^{2-})} \end{array}\right\} \quad (8)$$

It was solved using MATCAD 10.

The results of the conducted calculations are presented in Fig. 7 in the form of a calculated diagram of the homogeneity region of nanocrystalline PdO films. As the figure shows, the values of the oxidation temperature T_{ox} are presented as a function of deviation from the stoichiometric ratio δ of the elements in the composition of nanocrystalline palladium (II) oxide films. The values δ were calculated for two different values of the radius of oxygen anion $R(O^{2-})$ = 0.124 nm and $R(O^{2-})$ = 0.140 nm known from previous works (Table. 2). The calculation of the values of deviation from stoichiometry δ using these values of radii of oxygen anion leads to very similar results (Fig. 7).

According to the calculation results, the nonstoichiometry area of nanocrystalline PdO films obtained using oxidation in oxygen is rather wide and varies in the range from $-0.20 + 0.04 \le \delta \le 0.12 + 0.04$ mol. f. (Fig. 6). As Fig. 7 shows, heterogeneous samples (Pd + PdO) synthesised at T_{ox} = 570 K and T_{ox} = 1120 K are

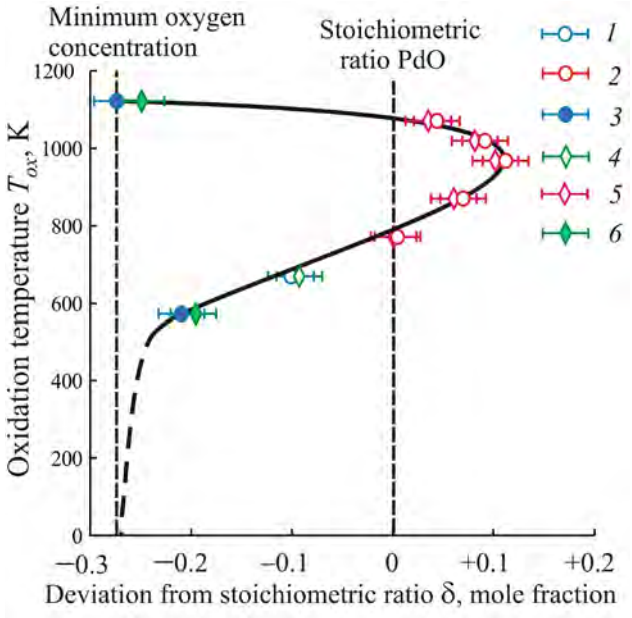

Fig. 7. The calculated model of the nonstoichiometry area of nanocrystalline palladium (II) oxide films prepared by oxidation in the oxygen atmosphere (O_2 partial pressure is 105–110 kPa); *1*, *4* – homogeneous PdO samples with a deficiency of oxygen atoms; *2*, *5* – homogeneous PdO samples with an excess of oxygen atoms; *3*, *6* – heterogeneous PdO + Pd samples; *1*, *2*, *3* – calculation for the ionic radius of oxygen O^{2-} $R(O^{2-})$ = 0.124 nm; *4*, *5*, *6* – calculation for the ionic radius of oxygen $R(O^{2-})$ = 0.140 nm.

characterised by the least content of oxygen atoms (the area of negative values of ô). In the latter case, nanocrystalline films show all the signs of thermal decomposition. With the same value of partial pressure O_2, an increase in the oxidation temperature from T_{ox} = 570 to T_{ox} = 970–1020 K leads to an increase in the concentration of oxygen atoms in nanocrystalline PdO films, which is accompanied by an anisotropic increase in the volume of the unit cell of the crystal structure (Fig. 3) and a decrease in the X-ray density (Fig. 4).

Generalisation of the experimental and calculation data obtained in the present work allows stating the strong influence of the oxidation temperature on the change in the concentration of oxygen atoms in nanocrystalline PdO films, which leads to the distortion of their crystal structure.

Altogether, the obtained experimental and calculated data indicate that the deviation from stoichiometry can be caused by point defects in the anion sublattice. As for nanocrystalline PdO films that were synthesised at T_{ox} = 570–670 K, a deficiency of oxygen atoms can be explained by the formation of oxygen vacancies V_O. It is likely that these vacancies are filled with oxygen atoms when the oxidation temperature is increased up to T_{ox} = 770 K. PdO samples obtained at T_{ox} = 870–1070 K are characterised by an excess of oxygen atoms in relation to the stoichiometry and minimal density values due to embedded interstitial atoms of oxygen O_i. Further increase in the oxidation temperature leads to a decrease in the concentration of oxygen atoms in the PdO films, which indicates the retrograde nature of the solidus line in this region of the composition and temperature (Fig. 7).

The results of the conducted calculations allow stating that single-phase nanocrystalline PdO films possess a two-sided homogeneity region in relation to the stoichiometric ratio of the components. The data obtained in the present work will contribute to the development of effective gas sensors with best functional parameters based on the nanostructures of palladium (II) oxide.

4. Conclusions

1. Based on X-ray analysis, it was established that the parameters of the tetragonal structure of nanocrystalline films of palladium (II) oxide monotonously increase with an increase in the oxidation temperature from T_{ox} = 570 K to T_{ox} = 970 K and decrease at T_{ox} > 970 K.

2. It was shown that the distortions of the tetragonal lattice of nanocrystalline films of palladium (II) oxide were mainly due to an increase in the value of parameter *a*.

3. Based on the obtained experimental and calculation data, an assumption was made that the distortions of the tetragonal lattice of nanocrystalline palladium (II) oxide films were caused by the incorporation of excess oxygen atoms.

4. Based on an assumption that the ionic component of the chemical bond is essential, we developed a calculation method for the nonstoichiometry area of nanocrystalline palladium (II) oxide films.

5. Based on the conducted calculations, we developed a model for the nonstoichiometry areas of nanocrystalline palladium (II) oxide films. It was shown that the nonstoichiometry area is two-sided in relation to the stoichiometric composition and is characterised by the retrograde solidus line.

Conflict of interests

The authors declare that they have no known competing financial interests or personal relationships that could have influenced the work reported in this paper.

References

1. Korotcenkov G. *Handbook of gas sensor materials. Properties, fdvantages and shortcomings for applications. Volume 1: Conventional approaches*. New York, Heidelberg Dordrecht London: Springer, New York, NY; 2013. 442 p. https://doi.org/10.1007/978-1-4614-7165-3

2. Yamazoe N. Toward innovations of gas sensor technology. *Sensors and Actuators B*. 2005;108: 2–14. https://doi.org/10.1016/j.snb.2004.12.075

3. Marikutsa A. V., Rumyantseva M. N., Gaskov A. M., Samoylov A. M. Nanocrystalline tin dioxide: Basics in relation with gas sensing phenomena. Part I. Physical and chemical properties and sensor signal formation. *Inorganic Materials*. 2015;51(13): 1329–1347. https://doi.org/10.1134/S002016851513004X

4. Marikutsa A. V., Rumyantseva M. N., Gaskov A. M., Samoylov A. M Nanocrystalline tin dioxide: Basics in relation with gas sensing phenomena. Part II. Active

centers and sensor behavior. *Inorganic Materials*. 2016;52(13): 1311–1338. https://doi.org/10.1134/S0020168516130045

5. Seiyama T., Kato A., Fujiishi K., Nagatani M. A new detector for gaseous components using semiconductive thin films. *Analytical Chemistry*. 1962;34(11): 1502–1503. https://doi.org/10.1021/ac60191a001

6. Korotcenkov G. Metal oxides for solid-state gas sensors: What determines our choice? *Materials Science and Engineering: B*. 2007;139(1): 1–23. https://doi.org/10.1016/j.mseb.2007.01.044

7. Toda K., Furue R., Hayami S. Recent progress in applications of graphene oxide for gas sensing: A review. *Analytica Chimica Acta*. 2015;878: 43–53. https://doi.org/10.1016/J.ACA.2015.02.002

8. Chin Boon Ong, Law Yong Ng, Abdul Wahab Mohammad. A review of ZnO nanoparticles as solar photocatalysts: Synthesis, mechanisms and applications. *Renewable and Sustainable Energy Reviews*. 2018;81: 536–551. https://doi.org/10.1016/j.rser.2017.08.020

9. Al-Hashem M., Akbar S., Morris P. Role of oxygen vacancies in nanostructured metal-oxide gas sensors: A Review. *Sensors Actuators B*. 2019;301: 126845. https://doi.org/10.1016/j.snb.2019.126845

10. Kim H.-J., Lee J.-H. Highly sensitive and selective gas sensors using *p*-type oxide semiconductors: Overview. *Sensors and Actuators B*. 2014;192: 607–627. https://doi.org/10.1016/j.snb.2013.11.005

11. Ryabtsev S. V., Ievlev V. M., Samoylov A. M., Kuschev S. B., Soldatenko S. A. Microstructure and electrical properties of palladium oxide thin films for oxidizing gases detection. *Thin Solid Film*s. 2017;636: 751–759. https://doi.org/10.1016/j.tsf.2017.04.009

12. García-Serrano O., López-Rodríguez C., Andraca-Adame J. A., Romero-Paredes G., Pena-Sierra R. Growth and characterization of PdO films obtained by thermal oxidation of nanometric Pd films by electroless deposition technique. *Materials Science and Engineering B*. 2010;174(1-3): 273–278. https://doi.org/10.1016/j.mseb.2010.03.064

13. Ryabtsev S. V., Shaposhnik A. V., Samoylov A. M., Sinelnikov A. A., Soldatenko S. A., Kushchev S. B., Ievlev V. M. Thin films of palladium oxide for gas sensors. *Doklady Physical Chemistry*. 2016;470(2): 158–161. https://doi.org/10.1134/s0012501616100055

14. Samoylov A., Ryabtsev S., Shaposhnik A., Kuschev S., Soldatenko S., Ievlev V. Palladium oxide thin film for oxidizing gases detecting. In: *The 16-th International Meeting on Chemical Sensors IMCS 2016. Jeju, Jeju Island, Korea, July 10 – 13, 2016: Final Program & Absrtacts Book*. Korea: 2016. 96 p.

15. Ryabtsev S. V., Iyevlev V. M., Samoylov A. M., Kuschev S. B., Soldatenko S. A. Real microstructure and electrical properties of palladium oxide thin films for oxidizing gases detecting. In: *Science and Application of Thin Films, Conference & Exhibition (SATF-2016) Çeşme, Izmir, Turkey, September 19–23, 2016. Book of Abstract: Izmir Institute of Technology*. Izmir: 2016. 44 p.

16. Ievlev V. M., Ryabtsev S. V., Shaposhnik A. V., Samoylov A. M., Kuschev S. B., Sinelnikov A. A. Ultrathin films of palladium oxide for oxidizing gases detecting. *Procedia Engineering*. 2016;168: 1106–1109. https://doi.org/10.1016/j.proeng.2016.11.357

17. Ievlev V. M., Ryabtsev S. V., Samoylov A. M., Shaposhnik A. V., Kuschev S. B., Sinelnikov A. A. Thin and ultrathin films of palladium oxide for oxidizing gases detection. *Sensors and Actuators B*. 2018;255 (2): 1335–1342. https://doi.org/10.1016/j.snb.2017.08.121

18. Samoylov A. M., Ryabtsev S. V., Popov V. N., Badica P. Palladium (II) oxide nanostructures as promising materials for gas sensors. In: *Novel nanomaterials synthesis and applications*. George Kyzas (ed.). UK, London: IntechOpen; 2018. pp. 211–229. http://dx.doi.org/10.5772/intechopen.72323

19. *Diagrammy sostoyaniya dvoinykh metallicheskikh sistem: Spravochnik: v 3 tomakh* [Phase diagrams of binary metal systems: Handbook: in 3 volumes]. Lyakishev N. P. (ed.) Moscow: Metallurgy Publ.; 1996–2000. (In Russ.)

20. Samoylov A. M., Ivkov S. A., Pelipenko D. I., Sharov M. K., Tsyganova V. O., Agapov B. L., Tutov E. A., Badica P. Structural changes in palladium nanofilms during thermal oxidation. *Inorganic Materials*. 2020;56(10): 1020–1026. https://doi.org/10.1134/S0020168520100131

21. Hammond C. The basics of crystallography and diffraction. Fourth edition. International Union of Crystallography. Oxford University Press; 2015. 519 p. https://doi.org/10.1093/acprof:oso/9780198738671.003.0009

22. *ASTM JCPDS - International Centre for Diffraction Data*. © 1987–2009. JCPDS-ICDD. Newtown Square, PA 19073. USA.

23. Grier D., McCarthy G., North Dakota. State University, Fargo, N. Dakota, USA, ICDD Grant-in-Aid, JCPDS-ICDD, 1991. Card no. 43-1024.

24. Kumar J., Saxena R. Formation of NaCl- and Cu_2O-type oxides of platinum and palladium on carbon and alumina support films. *Journal of the Less Common Metals*. 1989;147(1): 59–71. https://doi.org/10.1016/0022-5088(89)90148-3

25. Wiberg, E., Wiberg, N., Holleman, A. F. *Inorganic Chemistry. 1st English Edition*. San Diego: Academic Press; Berlin: New York: De Gruyter; 2001. 1884 p.

26. Al-Hashem M., Akbar S., Morris P. Role of oxygen vacancies in nanostructured metal-oxide gas sensors: A Review. *Sensors and Actuators B*. 2019;301: 126–154. https://doi.org/10.1016/j.snb.2019.126845

27. Ugay Ya. A. *Neorganicheskaya khimiya* [Inorganic chemistry]. Moscow: Vysshaya shkola Publ.; 1989. 483 p. (In Russ.)

28. Greenwood N. N., Earnshaw A. *Chemistry of the Elements, 2nd Ed.* Oxford: A division of Reed Educational and Professional Publishing Ltd., 1998. 1341 p.

29. Goncharov E. G., Semenova G. V., Ugay Ya. A. *Khimiya poluprovodnikov* [Chemistry of semiconductors]. Voronezh: Voronezh State University Publ.; 1995. 272 p. (In Russ.)

30. https://www.webelements.com/palladium/atom_sizes.html WebElements: The periodic table on the WWW [www.webelements.com] Copyright 1993–2018 Mark Winter [The University of Sheffield and Web Elements Ltd, UK]. All rights reserved.

31. Shannon R. D. Revised effective ionic radii and systematic studies of interatomic distances in halides and chalcogenides. *Acta Crystallographica Section A*. 1976;32(5): 751–767. https://doi.org/10.1107/s0567739476001551

32. Emsley J. *The elements*. *3-d Edition*. United Kingdom, Oxford: Clarendon Press; 1998. 298 p.

Information about the authors

Alexander M. Samoylov, DSc in Chemistry, Associate Professor, Professor at the Department of Materials Science and the Industry of Nanosystems, Voronezh State University, Voronezh, Russian Federation; e-mail: samoylov@chem.vsu.ru. ORCID iD: https://orcid.org/0000-0003-4224-2203.

Dmitry I. Pelipenko, post-graduate student at the Department of Materials Science and the Industry of Nanosystems, Voronezh State University, Voronezh, Russian Federation; e-mail: pelipencko.dmitry@yandex.com. ORCID iD: https://orcid.org/0000-0002-7698-7249

Natalia S. Kuralenko, student, Faculty of Chemistry, Department of Materials Science and the Industry of Nanosystems, Voronezh State University, Voronezh, Russian Federation; e-mail: nataliprosto99@gmail.com. ORCID iD: https://orcid.org/0000-0001-9604-1058

All authors have read and approved the final manuscript.

Received 09 February 2021; Approved after reviewing 15 February 2021; Accepted 15 March 2021; Published online 25 March 2021.

Translated by Marina Strepetova
Edited and proofread by Simon Cox